Theor Chem Acc (2000) 104:312–316
DOI 10.1007/s002140000157

Theoretical
Chemistry Accounts

Regular article

Intramolecular coupling study on nonlinear optical signals

J. L. Paz, T. Cusati, M. C. Salazar, A. J. Hernández

Departamento de Química, Universidad Simón Bolívar, Apartado 89000, Caracas 1080[a], Venezuela

Received: 17 September 1999 / Accepted: 9 March 2000 / Published online: 21 June 2000

Abstract. In this contribution, we have introduced intramolecular coupling in order to study possible modifications in the topology of the resonances associated with the four-wave mixing signal emerging as a consequence of incorporating the permanent dipole moments when the rotating-wave approximation is not included.

Key words: Intramolecular coupling – Four-wave mixing

1 Introduction

The two-state model for the characterization of molecules interacting with a classical electromagnetic field has proven to be useful in molecular spectroscopy and nonlinear optics [1, 2]. Generally, these two states are considered to interact with each other through the external field. Our present model consists of two electronic states whose potential-energy curves are described as two displaced harmonic potentials. In this study, we investigate topological modifications introduced in the four-wave mixing signal for a homogeneously broadened two-level system, including a simple scheme for the vibrational structure and the intramolecular coupling interactions and considering the presence of molecular electronic states with nonzero permanent dipole moments. We carefully examine how the intramolecular coupling may affect properties found for systems in which such a coupling does not occur. Our effective two-level system of vibronic states is described in Fig. 1. The curves are displaced horizontally by R_0 and vertically by V_0, the ground-state vibrational energies by E_{10} and E_{20} for each potential, and the vibrational wavefunctions by ϕ_{10} and ϕ_{20}, respectively. This description of intercrossing electronic states corresponds to the so-called diabatic or uncoupled representation [3].

A residual perturbation, $\tilde{H}$, coupling these electronic states can be also included. Consequently, the previous curves can be now separated according to the avoided-crossing rule as depicted in Fig. 2, where these new eigenstates of the electronic Hamiltonian belong now to the so-called adiabatic or coupled representation and its shape depends on the value of the non-diagonal matrix element of $\tilde{H}$ (denoted in Fig. 2 by v). Here, E^+ and E^- denote the resulting vibronic energies after inclusion of the coupling $\tilde{H}$, and the situation illustrated in Fig. 2 corresponds to situation where the diabatic picture renders a good description for the vibronic states.

Correspondence to: J. L. Paz

2 Intramolecular coupling model

In the present model, the Hamiltonian associated with the molecular system can be written as $H = H_0 + \tilde{H}$, where H_0 represents two harmonic oscillators uncoupled from each other and $\tilde{H}$ corresponds to a residual term (depending only on the electronic coordinates) which induces the intramolecular coupling. The two energy levels and the corresponding eigenfunctions involved can be then written as

$$E^{\pm} = \frac{1}{2}\left\{(E_{1j} + E_{2k}) \pm \left[(E_{1j} - E_{2k})^2 + 4v^2|\langle\phi_{1j}|\phi_{2k}\rangle|^2\right]^{1/2}\right\} \quad (1)$$

and

$$\Psi^{\pm}(r;R) = C_{1j}^{\pm}\left[\psi_1(r;R)\phi_{1j}(R) \pm A_{jk}^{\pm}\psi_2(r;R)\phi_{2k}(R)\right] , \quad (2)$$

where r and R correspond to the electronic and nuclear coordinates and where the following equalities hold: $E_{1j} = (j + 1/2)\hbar\omega$, $E_{2k} = (k + 1/2)\hbar\omega + V_0$; $C_{1j}^{\pm} = \left[1 + \left(A_{jk}^{\pm}\right)^2\right]^{-1/2}$ with $A_{jk}^{\pm} = \left(E_{1j} - E^{\pm}\right)/\langle\phi_{1j}|\phi_{2k}\rangle v$.

In our case, v represents the nondiagonal matrix element of $\tilde{H}$ between the electronic wavefunctions $\psi_1(r;R)$ and $\psi_2(r;R)$. The usual criteria of weak-, intermediate- and strong-coupling cases apply here:

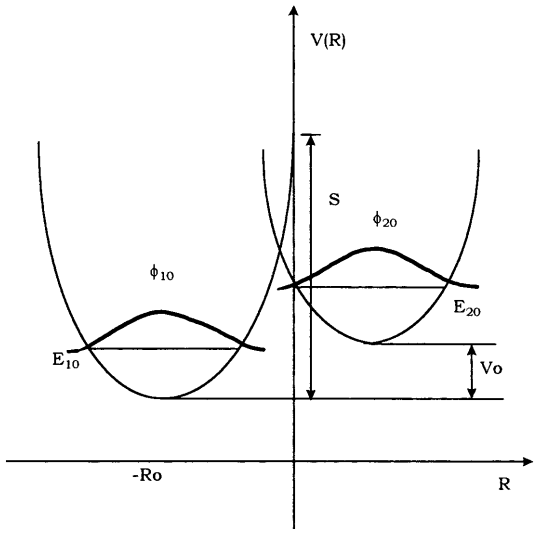

Fig. 1. Diabatic representation. The ground-state vibrational energies (E_{10} and E_{20}) for each harmonic potential and corresponding vibrational wavefunctions (ϕ_{10} and ϕ_{20}) are represented. The minima of the two potentials are displaced vertically in energy by V_0 and horizontally by the distance R_0

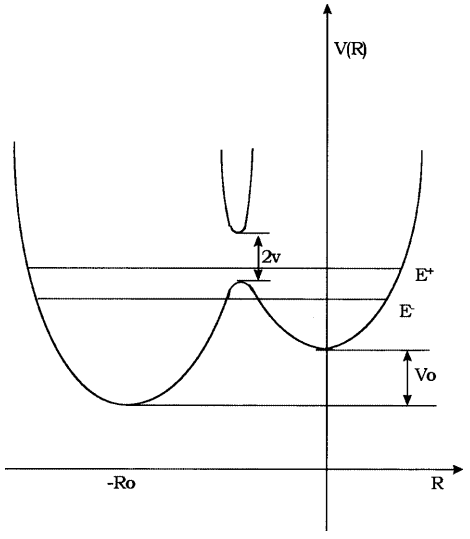

Fig. 2. Adiabatic representation. The residual perturbation giving rise to the separation of the two harmonic curves (represented in Fig. 1) is depicted according to an avoided-crossing rule

$v \ll S\hbar\omega/4$, $v \approx S\hbar\omega/4$, and $v \gg S\hbar\omega/4$, respectively, where $S = (m\omega/\hbar)R_0^2$, with m being the mass associated with the vibrational mode described by the nuclear coordinate R and where R_0 represents the coordinate separation in the two-minima electronic potentials [4].

In our model, the transition and permanent dipole moments between the states Ψ^- and Ψ^+ can be written as

$$\mu_{-+} = -C_{1j}^{-}C_{1j}^{+}\left[A_{jk}^{-}A_{jk}^{+}\mu_{22}(0) + \mu_{11}(-R_0)\right] - C_{1j}^{-}C_{1j}^{+}\mu_{12}(-R_0)\langle\phi_{1j}|\phi_{2k}\rangle\left(A_{jk}^{+} + A_{jk}^{-}\right) \quad (3)$$

and

$$\mu_{ii} = \left(C_{1j}^{i}\right)^2\left[\left(A_{jk}^{i}\right)^2\mu_{22}(0) + \mu_{11}(-R_0)\right] - 2\left(C_{1j}^{i}\right)^2\mu_{12}(-R_0)\langle\phi_{1j}|\phi_{2k}\rangle\left(A_{jk}^{i}\right), \quad (4)$$

with $i = -$ or $+$.

We have also considered nonzero permanent dipole moments associated with the states described by the uncoupled states ψ_1 and ψ_2, respectively, described by

$$\mu_{ij}(R) = \int \psi_i^*(r;R)\hat{\mu}\psi_j(r;R)d^3r \ , \quad (5)$$

where $\hat{\mu}$ is the total electronic dipole moment operator and $i, j = 1, 2$. These moments μ_{ij} are evaluated at the nuclear equilibrium distances corresponding to each uncoupled electronic state, i.e., $\mu_{11}(-R_0)$, $\mu_{22}(0)$, and (by the Franck–Condon principle) $\mu_{12}(-R_0)$. The vibrational overlap factors $\langle\phi_{1j}|\phi_{2k}\rangle$ in the above expression can be then evaluated according to the Pekarian formula [4] as $\langle\phi_{10}|\phi_{2k}\rangle = \frac{(-1)^k}{(k!)^{1/2}}S^{k/2}\exp(-S/4)2^{-k/2}$ for the case $j = 0$.

3 Four-wave-mixing signal and macroscopic nonlinear local polarization

We presently describe the time-dependent interaction of a molecule with a total external field and with a heat reservoir using the Liouville formalism [5] and the conventional optical Bloch equations in the semiclassical approximation:

$$\dot{\rho}(t) = \sigma(t)\rho(t) + \mathscr{R} \ , \quad (6)$$

where

$$\rho(t) = \begin{pmatrix} \rho_{-+} \\ \rho_{+-} \\ \rho_{\mathrm{D}} \end{pmatrix}; \ \sigma(T) = \begin{pmatrix} A & 0 & i\Omega \\ 0 & B & i\Omega^* \\ 2i\Omega & -2i\Omega & -1/T_1 \end{pmatrix}; \quad \mathscr{R} = \begin{pmatrix} 0 \\ 0 \\ \rho_{\mathrm{D}}^{(0)}T_1^{-1} \end{pmatrix}$$

and where $A = -\left[i(\omega_0 - \gamma) + T_2^{-1}\right]$ and $B = [i(\omega_0 - \lambda) - T_2^{-1}]$. Here, $|\Omega|$ and $|\lambda|$ represent the radiative interaction among the incident plane wave, $\vec{E}(t)$, characterized by the Rabi frequency $\Omega = \vec{\mu}_{-+}\vec{E}(t)/\hbar$, and $\lambda = \vec{\xi}\vec{E}(t)/\hbar$, with $\vec{\xi} = \vec{\mu}_{--} - \vec{\mu}_{++}$, where $\vec{\mu}_{-+}$ and $\vec{\xi}$ are the transition moments and difference between the permanent dipole moments for the coupled states, respectively, T_1 and T_2 are the longitudinal and transversal relaxation times, and ω_0 represents the Bohr frequency of the molecular two-level system. In the present model, we introduce the four- wave-mixing (FWM) spectroscopy technique, where the solution consists of a nonabsorbent solvent and solute molecules having an electronic transition in resonance with the electromagnetic fields. In this experimental technique, two incident laser beams (a pump and a probe) generate a signal at a mixed frequency and wave vector. The nonlinear signal frequency and wave vector are related by $\omega_3 = 2\omega_1 - \omega_2$ and $\vec{k}_3 \approx 2\vec{k}_1 - \vec{k}_2$,

where the subscripts 1, 2, and 3 refer to pump, probe, and signal field, respectively. In the FWM technique, we can also write the intensity in the local regime of propagation for the generated signal by $I_{\mathrm{FWM}} = c\varepsilon|\vec{P}_{\mathrm{H}}(t)|^2/8\pi$, with $\vec{P}_{\mathrm{H}}(t)$ being the homogeneous macroscopic polarization, expressed by

$$\vec{P}_{\mathrm{H}}(t) = NTr[\rho(t)\vec{\mu}] \ , \tag{7}$$

where N represents the chemical concentration of the absorbent molecules. Taking into account the antiresonant terms and neglecting the rotating-wave approximation, Eq. (7) can be solved perturbatively to second order in the pump beam (ω_1) and first order in the probe beam (ω_2) to give the following expression of the frequency Fourier components of the induced polarization for the homogeneous spectral linewidth:

$$\vec{P}(\omega_3) = N\langle\rho_{++}(\omega_3)\vec{\mu}_{++} + \rho_{--}(\omega_3)\vec{\mu}_{--} + \rho_{-+}(\omega_3)\vec{\mu}_{+-} + \rho_{+-}(\omega_3)\vec{\mu}_{-+}\rangle_\theta \ , \tag{8}$$

where the angled brackets correspond to an average over the distribution of molecular orientation, θ. Here, $\rho_{ii}(\omega_3)(i = -,+)$ represents the Fourier component of the population that oscillates at frequency ω_3, and $\rho_{-+}(\omega_3)$ and $\rho_{+-}(\omega_3)$ represent the Fourier components of the coherences oscillating at the same frequency. In the steady-state approximation [6] and calculating the different components (coherences and populations) of the reduced density matrix at the optical frequency of interest, we are led to the following expression for the polarization:

$$\begin{aligned} P(\omega_3) = N\Bigg\{ & i\rho_{\mathrm{D}}^{(0)}\mu_{-+}\Bigg[\frac{1}{(D_3^+)^*}\Bigg[2\Omega_1^2\Omega_2^*\Bigg[\frac{1}{\Gamma}\Bigg(\frac{1}{D_2^+} \\ & + \frac{1}{D_1^-} + \frac{1}{(D_2^-)^*} + \frac{1}{(D_1^+)^*}\Bigg) + \frac{1}{\gamma}\Bigg(\frac{1}{D_1^-} + \frac{1}{(D_1^+)^*}\Bigg)\Bigg] \\ & + \frac{\phi_1^2\Omega_2^*}{(D_\Delta^+)^*(D_\Delta^-)^*} + \frac{\phi_1\phi_2^*\Omega_1}{(D_1^+)^*}\Bigg(\frac{1}{(D_\Delta^+)^*} + \frac{1}{(D_5^+)^*}\Bigg)\Bigg]\Bigg] \\ & - \frac{1}{D_3^-}\Bigg[2\Omega_1^2\Omega_2^*\Bigg[\frac{1}{\Gamma}\Bigg(\frac{1}{D_2^+} + \frac{1}{D_1^-} + \frac{1}{(D_2^-)^*} + \frac{1}{(D_1^+)^*}\Bigg) \\ & + \frac{1}{\gamma}\Bigg(\frac{1}{D_1^-} + \frac{1}{(D_1^+)^*}\Bigg)\Bigg] + \frac{\phi_1^2\Omega_2^*}{(D_\Delta^-)^*(D_2^+)^*} \\ & + \frac{\phi_1\phi_2^*\Omega_1}{(D_1^-)}\Bigg(\frac{1}{(D_\Delta^-)} + \frac{1}{(D_5^-)}\Bigg)\Bigg] \\ & + \frac{i\rho_{\mathrm{D}}^{(0)}\xi}{\beta}\Bigg[\Omega_1^2\phi_2^*\Bigg(\frac{1}{D_1^-D_\Delta^-} - \frac{1}{(D_1^+)^*(D_\Delta^+)^*}\Bigg) \\ & + \Omega_1\Omega_2^*\phi_1\Bigg(\frac{1}{D_\Delta^-D_2^+} + \frac{1}{D_5^-D_1^-} - \frac{1}{(D_\Delta^+)^*(D_2^-)^*} \\ & - \frac{1}{(D_5^+)^*(D_1^+)^*}\Bigg)\Bigg]\Bigg\} \ , \end{aligned} \tag{9}$$

where

$$\begin{aligned} & D_j^\pm = \frac{1}{T_2} + i(\omega_0 \pm \omega_j) \quad \text{for } j = 1,2,3, \\ & \Gamma = \frac{1}{T_2} - i(\omega_1 - \omega_2),\ D_5^\pm = \frac{1}{T_2} + i(\omega_0 \pm 2\omega_1) \\ & \gamma = \frac{1}{T_1} - 2i\omega_1, \beta = \frac{1}{T_1} - i\omega_3,\ D_\Delta^\pm = \frac{1}{T_2} + i(\omega_0 \pm \Delta) \ . \end{aligned}$$

Generally, the FWM spectrum is obtained as a function of the frequency of one of the incident beams tuned on and off the resonant frequency. Studying the characteristics of these spectra is important for understanding the properties of the nonlinear process that generates the signal and for the optimization of the method of measuring the population and phase relaxation times, T_1 and T_2, respectively. In this article we study the topological characteristics of the signal in a frequency space given by $\Delta_1 = \omega_1 - \omega_0$ and $\Delta_2 = \omega_2 - \omega_0$, where the intensity of the FWM signal in the present local homogeneous third-order model is proportional to the square modulus of the complex polarization. A better resolution of the signal's spectra in frequency space is obtained by means of the following normalized expression:

$$I_{\mathrm{FWM}}(\omega_3;\Delta_1,\Delta_2) = \frac{|\vec{P}(\omega_3;\Delta_1,\Delta_2,\tilde{\vec{\xi}})|^2}{|\vec{P}(\omega_3;\Delta_1=\Delta_2=0,\tilde{\vec{\xi}})|^2} \ , \tag{10}$$

where now $\tilde{\vec{\xi}} = \vec{\xi}$ for the coupled states and $\tilde{\vec{\xi}} = \vec{d}$ for uncoupled states, according to the definition $\vec{\xi} = \vec{\mu}_{--} - \vec{\mu}_{++}$ and $\vec{d} = \vec{\mu}_{22} - \vec{\mu}_{11}$, respectively. For all calculations, we chose green malachite dye with a resonance frequency $\omega_0 = 3.0628 \times 10^{15}\,\mathrm{s}^{-1}$ and values of $T_1 = T_2 = 1.3 \times 10^{-13}\,\mathrm{s}$ and having transition and permanent dipole moment values of $\mu_{12} = \mu_{21} = 0.1\,\mathrm{D}, \mu_{11} = 1.0\,\mathrm{D}$, and $\mu_{22} = 1.3\,\mathrm{D}$. These parameters correspond to typical large organic dyes, which we furthermore consider as solutions of aligned solute molecules (dimers) with intramolecular (intermolecular) couplings. Furthermore, and for the sake of simplicity, we will only consider the situation in which the permanent and transition dipole moments are aligned with the external electric field. This assumption is frequently used [7].

We have studied in previous work the effects of these permanent dipole moments in the absence of the rotating-wave approximation, which generates new peaks (different from the ones obtained at zero permanent dipole moments) associated with the FWM signal for a homogeneous two-level system [8]. All the results of previous work by Bessega et al. [8] and Paz et al. [9], which included the permanent dipole moments of the system without intramolecular coupling, were reproduced here as limiting cases for spectral regions of reduced detuning frequency.

The intensity of the FWM signal predicted in the present model as a function of the pump and probe detunings is depicted in Fig. 3, where the intramolecular coupling is included in the frequency intervals $(-\omega_0, \omega_0)$ for ω_1 and $(-2\omega_0, 2\omega_0)$ for ω_2. It is important to note here that it is always possible to obtain a frequency

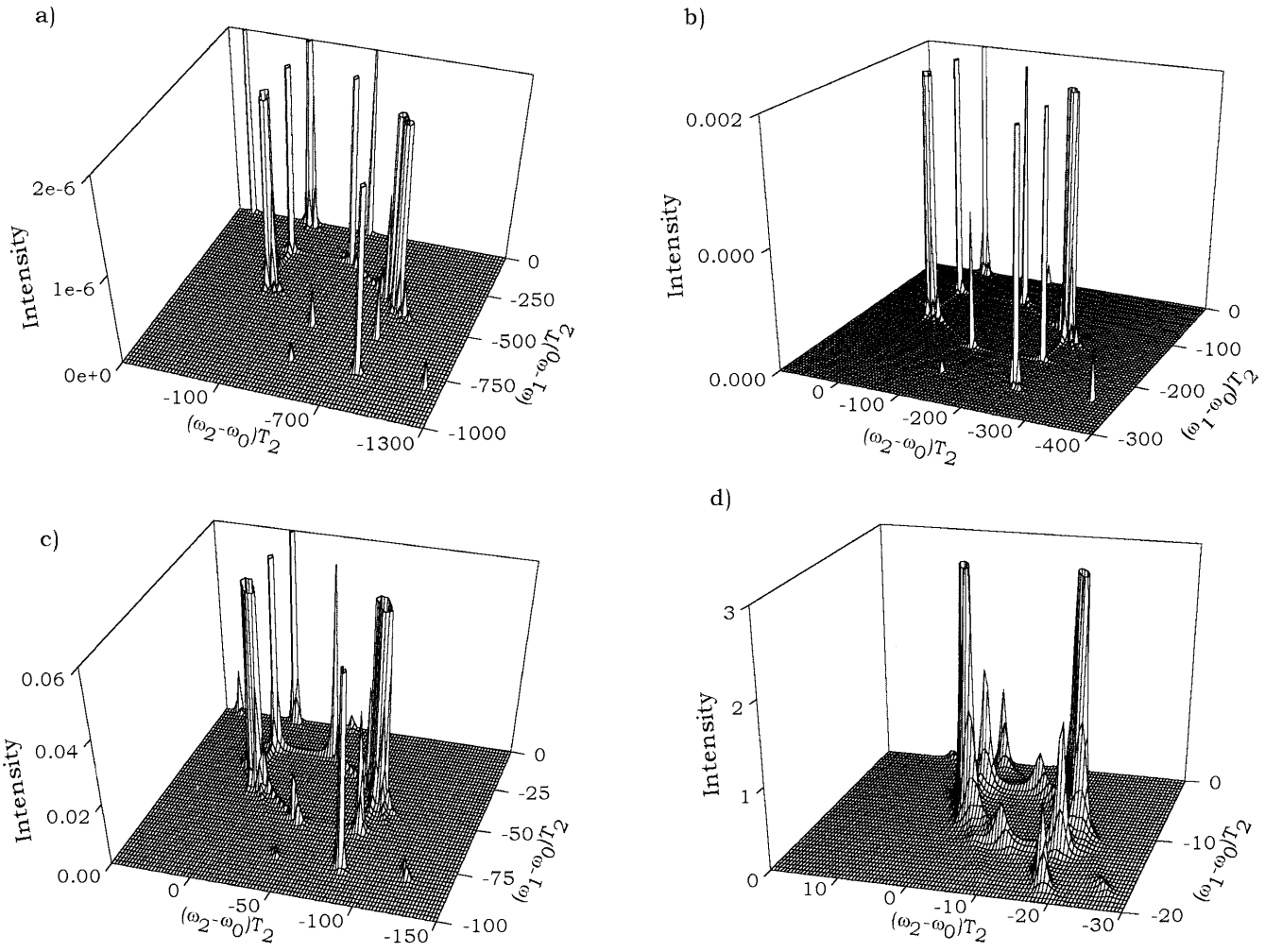

Fig. 3. Intensity of the four-wave-mixing signal as a function of the pump $(\omega_1 - \omega_0)T_2$ and probe $(\omega_2 - \omega_0)T_2$ detuning, taking into account the intramolecular coupling for cases **a** $V_0 = 1$, **b** $V_0 = 0.3$, **c** $V_0 = 0.1$ and **d** $V_0 = 0.01$ The value of the intramolecular coupling parameter is 0.01 in all cases

spectrum with characteristics equivalent to the previously studied cases using the present adiabatic representation by considering similar $\tilde{\omega}_0$ for the uncoupled basis. We can observe from Fig. 3 a shifting to lower detuning values of the different resonances involved with a decrease in the coupling parameters. For instance, the decrease in the parameter V_0 represented by the sequence from Fig. 3a–d, generates a cluster formed by six out of a total of 12 peaks (Fig. 3d). As is highly evident from Fig. 3d, our final spectrum has 12 resonance-structure configurations carrying the intensity symmetry and the symmetry of the detuning coordinates. Equivalent behavior can also occur when V_0 is constant and the parameter v is decreased.

4 Final comments

The model presented in this contribution represents a generalization of the conventional local models proposed to date in the literature. In general, these conventional studies do not take into account the permanent molecular dipole moments and they usually leave out the anti-resonant terms neglected by using the rotating-wave approximation. Additionally, in this sutdy we have incorporated the intramolecular coupling and its effect on the topological description associated with the FWM optical signal. We have also shown that working in frequency space is very useful for the analysis of the topology of the nondegenerate FWM signal. More details concerning to the localization of these resonances with respect to the coupling parameters, the relation between their frequency and the local nonlinear polarization, and details concerning the topological modification of these peaks by including spatial propagation of the fields, high-order effects in the electromagnetic fields, stochastic effects of the solvent, stochastic effects of the phase associated with the fields, and the connection between the reduced polarization and the photonics process of each resonance are to be published elsewhere.

Acknowledgements. The present work was supported by the Consejo Nacional de Investigaciones Científicas y Tecnológicas (CONICIT) (grant G-97000593) and by the Decanato de Investigaciones of the Universidad Simón Bolívar (grant GID-13).

References

1. Meystre O, Sargent III M (1990) Quantum optics. Springer, Berlin Heidelberg New York
2. Boyd RW (1992) Nonlinear optics. Academic, New York
3. Shatz GC, Ratner MA (1993) Quantum mechanics in chemistry. Prentice Hall, New York
4. Paz JL, García-Sucre M, Squitieri E, Mujica V (1994) Chem Phys Lett 217: 333
5. Blum K (1981) Density matrix theory and applications. Plenum, New York
6. Bloembergen N (1996) Nonlinear optics. World Scientific, London
7. (a) Bavli R, Band YB (1991) Phys Rev A 43: 507; (b) Bavli R, Band YB (1991) Phys Rev A 43: 5039, (c) Bavli R, Band YB (1991) Phys Rev A 43: 5044
8. Bessega MC, Paz JL, Hernández AJ, Cárdenas AE (1995) Phys Lett A 206: 305
9. Paz JL, Bessega MC, Cárdenas AE, Hernández AJ (1995) J Phys B At Mol Opt Phys 28: 5377